

Single-chain conformation of carboxylated schizophyllan, a triple helical polysaccharide, in dilute alkaline aqueous solution

slettet: o

Yu Tomofuji^a, Kazuto Yoshiba^{b,*}, Bjørn E. Christensen^c, and Ken Terao^{a,*}

^a Department of Macromolecular Science, Graduate School of Science, Osaka University, 1-1 Machikaneyama-cho, Toyonaka, Osaka 560-0043, Japan.

^b Division of Molecular Science, Graduate School of Science and Technology, Gunma University, 1-5-1 Tenjin-cho, Kiryu, Gunma, 376-8515, Japan.

^c NOBIPOL, Department of Biotechnology and Food Science, Norwegian University of Science and Technology (NTNU), Trondheim NO-7491, Norway

* Corresponding authors.

E-mail addresses: yoshiba@gunma-u.ac.jp (K. Yoshiba), kterao@chem.sci.osaka-u.ac.jp (K. Terao)

ABSTRACT

Synchrotron-radiation small-angle X-ray scattering measurements were carried out for a schizophyllan (SPG) sample with the weight-average molar mass M_w of 340 kg mol^{-1} and five carboxylated SPG (sclerox) samples with different degrees of substitution (DS) ranging from 0.18 to 0.45 in 200 mM aqueous NaOH including 10 mM NaCl to determine M_w , the second virial coefficient A_2 , the particle scattering function $P(q)$, and the radius of gyration $\langle S^2 \rangle$. Positive A_2 values indicated that this alkaline solvent was a good solvent for all polysaccharide samples investigated. The resultant M_w values ($\sim 100 \text{ kg mol}^{-1}$) were much smaller than that for the trimer in aqueous NaCl at neutral pH, indicating all SPG and sclerox samples dissolved as single chains in the alkaline solvent. Both $P(q)$ and $\langle S^2 \rangle$ data were consistently explained by the wormlike chain model. The obtained parameters were almost independent of DS. While

the chain stiffness (12 – 18 nm) in terms of the Kuhn segment length or twice the persistence length was similar to those for the other single chain polysaccharides, the helix pitch per residue (0.1 nm) was quite smaller than the trimer state (0.3 nm). This shrunken main-chain helical structure is most likely due to hydrophobic interactions between helical main chain and side groups.

slettet: the

Key Words: β -1,3-glucan, triple helix, single chain conformation, small-angle X-ray scattering, wormlike chain.

Highlights

Schizophyllan and scleroglucan dissolved in 200 mM aqueous NaOH as a single chain.

slettet: were

Dimensional properties are well explained by the wormlike chain model.

The chain stiffness of the single chain is similar to that for curdlan and cellulose.

slettet: C

The chain contour is shrunken to form locally winding helix.

1. Introduction

Multiple helices are among of the most abundant secondary structures of biopolymers, that is, DNA, collagen, and some polysaccharides. The double or triple helices dissociate to single chain in certain specific solvent conditions or at high temperatures. Since such polysaccharides, *e.g.*, xanthan or schizophyllan (SPG), are classified as homopolymers, the renatured structures in aqueous solution may be different from that of the native state. Indeed, xanthan, a double helical polysaccharide, forms hairpin-like double-helical structures consisting of a single polysaccharide molecule in dilute solution [1, 2], while double helical branched structures consisting of three or more xanthan molecules was observed when renatured at high concentrations [2-4]. Macromolecular cyclization behavior [5] was further found for SPG, a triple helical polysaccharide [6], and for a β -1,3-glucan produced by *Schizophyllum commune*, containing a β -1,6-linked glucose residue at every third main-chain residue [7, 8]. Furthermore, stable hetero-triple helices consisting of two SPG and one nucleotide molecules have been investigated [9-11] as a basis for constructing DNA delivery systems [12].

Although most research for such multiple helical biopolymers mainly focuses on the fixed helical structure, the single chain state is important to elucidate the mechanism of formation of the above-mentioned higher order structures. For example, both the chain conformation and hydration behavior of the single chain are definitely important for the thermal stability of triple-helical collagen model peptides [13, 14]. In the present study, we thus investigated single chain conformation of SPG in aqueous sodium chloride (NaCl) by means of synchrotron-radiation small-angle X-ray scattering (SAXS). The obtained conformational properties were quite different from that predicted for a simple random coil.

We thus extended this study to investigate carboxylated SPG (sclerox) [15] for which chemical structure is illustrated in Fig. 1. In the figure, m and n mean the number of the repeat

slettet: x

slettet: is

slettet: one

slettet: particular

slettet: some

slettet: to

slettet: a

slettet: one

slettet: it was

slettet: with

slettet: three

slettet: s

slettet: , is produced by the fungus *Schizophyllum commune*

slettet: were

slettet: to

slettet: may be also

slettet: mechanism

slettet: this

unit with oxidized and native side groups, respectively. This sclerox should have higher water-solubility due to ionized groups. Indeed, it was reported that triple helical structure of sclerox tends to be untied in aqueous media by means of the X-ray scattering data [16] even at neutral pH. We recently revealed that relatively long sclerox chains retain the triple helical structure in aqueous NaCl at neutral pH, while the main chain is much more flexible than the original SPG in the same solvent [17]. Both the characteristics of the triple helix formation and polyelectrolyte nature of sclerox are of interest as the delivery system *in vivo*.

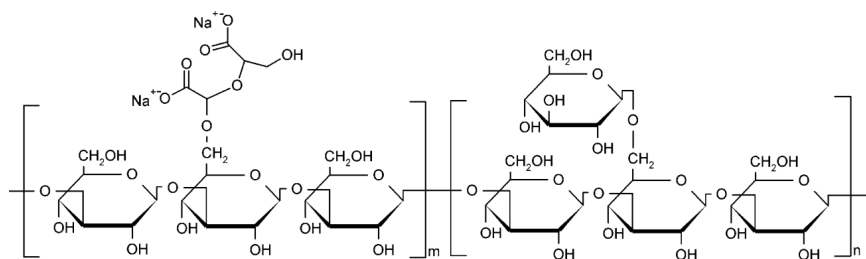


Fig. 1. Chemical structure of carboxylated schizophyllan (sclerox). Reprinted from ref [17], Copyright (2017), with permission from Elsevier.

2. Experimental section

2.1. Preparation of samples

Two SPG samples, **SPG-340K** and **SPG-540K**, were prepared from a SPG sample (Mitsui Sugar Co., Tokyo, Japan) by fractional precipitation in the manner reported previously [18]. Two step oxidation was conducted with NaIO_4 and NaClO_2 in aqueous solution to obtain sclerox samples. The detailed procedures [js](#) reported elsewhere [19]. We chose two sclerox samples, **SC18-340K** and **SC45-340K** from **SPG-340K** and three sclerox samples, **SC22-540K**, **SC24-540K**, and **SC43-540K** from **SPG-540K**. The degree of substitution (DS) defined as $m / (m + n)$ was determined by

slettet: s

slettet: were

potentiometric titration with 0.01 M aqueous NaOH containing 0.1 M NaCl after the deionization with an ion-exchange resin Amberlite IR-120B (Organo Co., Tokyo, Japan). The obtained DS ranges between 0.18 and 0.45. Taking into consideration that the molar mass $3M_0$ of the repeat unit of SPG and fully substituted sclerox are 0.649 kg mol⁻¹ and 0.693 kg mol⁻¹, respectively, the average molar mass M_0 per main chain saccharide unit is calculated to be 0.216 kg mol⁻¹ for SPG and 0.219 – 0.223 kg mol⁻¹ for the current sclerox samples.

2-2. *Size-exclusion chromatography combined with multi-angle light scattering (SEC-MALS)*

SEC-MALS measurements were made on **SPG-340K**, **SPG-540K**, **SC18-340K**, **SC45-340K**, **SC22-540K**, **SC24-540K**, and **SC43-540K** to determine the weight-average molar mass M_w and the dispersity index \mathcal{D} defined as the ratio of M_w to the number-average molar mass. A GPC-101 (Showa Denko KK., Kanagawa, Japan) chromatography system, a DAWN HELEOS II (Wyatt technology Co., USA) MALS detector, and a differential refractometer (RI) were used with serially connected SEC columns, a guard column (OHpak SB-G, Showa Denko) and two SEC columns (OHpak SB-806M-HQ, Showa Denko) set in a column oven at 40 °C. The flow rate of the eluent, 100 mM aqueous NaCl, was set to be 1.0 mL min⁻¹; we note that triple helical structure was retained in the solvent [19]. The MALS and RI detectors operated at room temperature around 25 °C were calibrated with a poly(ethyleneoxide) sample **SE-5** (TOSOH Co. Ltd., Tokyo, Japan) for which M_w and \mathcal{D} are 44.2 kg mol⁻¹ and 1.03, respectively. The experimental details and data analysis are the same as that in our previous paper [19].

2-3. *Small angle X-ray scattering (SAXS)*

SAXS measurements were carried out at the BL40B2 beamline in SPring-8 (Hyogo, Japan) for **SPG-340K**, **SC18-340K**, **SC45-340K**, **SC22-540K**, **SC24-540K**, and **SC43-540K** in 200 mM aqueous NaOH containing 10 mM NaCl at 25 °C to determine the single chain conformation both of SPG and sclerox samples in the solvent. Aqueous solutions of a standard sample, **SE-5**, was also measured at 25 °C. The wavelength λ_0 of the incident X-ray, the camera length, and the accumulation time were chosen to be 0.10 nm, 4.2 m, and 60 s, respectively. The scattered X-ray was detected with a PILATUS3S 2M silicon pixel detector (DECTRIS, Baden, Switzerland). The diffraction pattern of silver behenate was used to determine the accurate camera length and the position of the direct beam on the detector. The scattering intensity at each pixel was calibrated by the direct beam intensity detected at the lower end of the capillary cell. The solvent intensity was subtracted from that of the solution. The resultant excess intensity data were circularly averaged by SAngler software [20] to determine the excess scattering intensity $\Delta I(q)$ as a function of the magnitude q of the scattering vector. The ratio K/R_q of the optical constant K to the Rayleigh ratio R_q at q was estimated from the following equation [21, 22].

$$\frac{R_q}{K} = M_{w,\text{PEO}} \left(\frac{\Delta z_{\text{PEO}}}{\Delta z} \right)^2 \left[\frac{c_{\text{PEO}}}{\Delta I_{\text{PEO}}(q)} \right]_{c_{\text{PEO}} \rightarrow 0, q \rightarrow 0} \Delta I(q) \quad (1)$$

Subscript PEO means the values for the standard sample, **SE-5**. Here, Δz is defined as

$$\Delta z = z - \bar{v} \rho_{e,s} \quad (2)$$

where z , v , and $\rho_{e,s}$ are the number of moles of electron per unit mass of the solute, the partial specific volume, and the electron density of the solvent, respectively. Assuming the literature v value for SPG (0.619 mL g^{-1} [6]), Δz is estimated to be 185 mol kg^{-1} for SPG and $181 - 183 \text{ mol kg}^{-1}$ for the sclerox samples.

3. Results and Discussion

The weight-average molar mass $M_{w,3}$ and the dispersity index \mathcal{D} of the trimer state of SPG and sclerox samples in 100 mM aqueous NaCl are summarized in Table 1 along with DS. The obtained $M_{w,3}$ values for the sclerox samples are the same order of the original sample but tend to decrease with increasing DS. Furthermore, the \mathcal{D} values for some carboxylated samples are larger than the original SPG samples. These results are consistent with our previous study on sclerox [19].

Table 1

Molecular characteristics of SPG and sclerox samples in aqueous media

Sample	DS	Trimer ^a		Unimer ^b		
		$M_{w,3} / \text{kg mol}^{-1}$	\mathcal{D}	$M_{w,1} / \text{kg mol}^{-1}$	$A_2 / 10^{-4} \text{ mol kg}^{-2} \text{ m}^3$	$\langle S^2 \rangle_z^{1/2} / \text{nm}$
SPG-340K	0	342	1.24	106	4.0	9.1
SPG-540K	0	544	1.41			
SC18-340K	0.18	335	1.13	85	0.7	8.5
SC45-340K	0.45	230	2.01	108	2.2	9.9
SC22-540K	0.22	525	1.29	97	1.5	9.4
SC24-540K	0.24	501	1.31	146	1.8	11.2
SC43-540K	0.43	486	1.51	101	2.1	9.5

^a From SEC-MALS in 100 mM aqueous NaCl. ^b From SAXS in 200 mM aqueous NaOH including 10 mM NaCl.

The square-root Zimm plots (Berry plots) for **SPG-340K** and **SC43-540K** in 200 mM aqueous NaOH including 10 mM NaCl are shown in Fig. 2 to discuss single chain conformation of the polysaccharide samples. The second virial coefficient A_2 and the z -average mean-square

radius of gyration $\langle S^2 \rangle_z$ were determined from the initial slopes of the extrapolated data points to $q^2 = 0$ and $c = 0$, respectively. The weight-average molar mass $M_{w,1}$ values calculated from the doubly extrapolated value to $q^2 = 0$ and $c = 0$ are listed in Table 1 along with A_2 and $\langle S^2 \rangle_z^{1/2}$. The obtained $M_{w,1}$ for **SPG-340K** is substantially the same as one third of the corresponding $M_{w,3}$, suggesting completely dissociation in the alkaline solvent. While the ratio $M_{w,3}/M_{w,1}$ is close to 3 for **SC24-540K**, the values for **SC18-340K**, **SC22-540K**, and **SC43-540K** are larger than 3 indicating scission of the main chain in the synthesis process. On the other hand, a smaller ratio (~ 2) was found for **SC45-340K**, suggesting partly dissociation even in the neutral solvent (100 mM aqueous NaCl). In any case, much lower $M_{w,1}$ value in the alkaline solvent than $M_{w,3}$ in the neutral solvent suggests that all SPG and sclerox molecules in the alkaline solvent are dissolved as a single molecules or unimers. The large positive A_2 values in the order of $10^{-4} \text{ mol kg}^{-2}\text{m}^3$ (or $\text{mol g}^{-2}\text{cm}^3$) supports good solubility in the alkaline solvent.

Kommenter [BEC1]: Maybe also other explanations. If degradation one would expect $M_{w,1}$ decrease with increasing DS, but this does not happen. $M_{w,1}$ is roughly the same except for SC24. A ratio above 3 could in principle also be due to aggregation in the triplex state

Kommenter [BEC2]: See comments in email

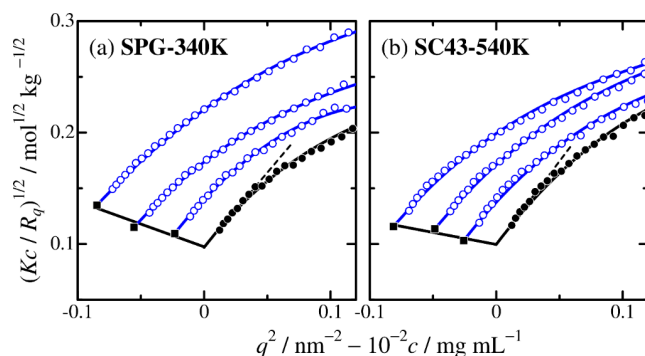


Fig. 2. Square-root Zimm plots (Berry plots) for **SPG-340K** (a) and **SC43-540K** (b) in 200 mM aqueous NaOH including 10 mM NaCl at 25 °C. Filled circles and squares, extrapolated values to $c = 0$ and $q^2 = 0$, respectively. Dashed lines indicate the initial slope to determine $\langle S^2 \rangle_z$.

Fig. 3 shows the Holtzer plot, that is, $qP(q)$ versus q for the SPG and sclerox samples in the alkaline solvent. The shape of the plots is typical for the wormlike chain for semiflexible polysaccharides [23]. We thus analyzed the data in terms of the touched-bead wormlike-chain model, $P(q)$ of which is expressed as [24-26]

$$P(q) = 9 \left(\frac{2}{qd_b} \right)^6 \left(\sin \frac{qd_b}{2} - \frac{qd_b}{2} \cos \frac{qd_b}{2} \right)^2 P_0(q) \quad (3)$$

where d_b and $P_0(q)$ are the bead diameter (a measure of the chain thickness) and the particle scattering function of the thin wormlike chain, respectively. $P_0(q)$ is written by the following equation

$$P_0(q) = \frac{2}{L^2} \int_0^L (L-t) I(\lambda^{-1}q; \lambda t) dt \quad (4)$$

Here, L is the contour length, λ^{-1} is the Kuhn segment length, and $I(\lambda^{-1}q; \lambda t)$ is the characteristic function, which can be calculated numerically by the approximate expression of Nakamura and Norisuye [27, 28]; note that λ^{-1} is the stiffness parameter and twice the persistence length. The three parameters, L , λ^{-1} , and d_b were determined unequivocally by means of a curve fitting procedure because appreciable horizontal region, ‘Holtzer plateau’ is found around $q = 1 \text{ nm}^{-1}$. The intramolecular excluded-volume effects are mostly negligible because the Kuhn segment number λL ranges between 2.6 and 4.3 [29, 30]. The upward deviation from the rod limiting values (dashed line) indicates the semiflexibility to identify the chain stiffness parameter. The resultant parameters are summarized in Table 2. It should be noted that the chain stiffness parameter may be overestimated due to the relatively large molar mass dispersity of sclerox

samples even though the actual \bar{D} value cannot be estimated correctly for sclerox in the alkaline solvent taking the above-mentioned chain degradation into consideration. The possible error on λ^{-1} is about 20 – 30 % when assuming $\bar{D} = 1.6$ [23].

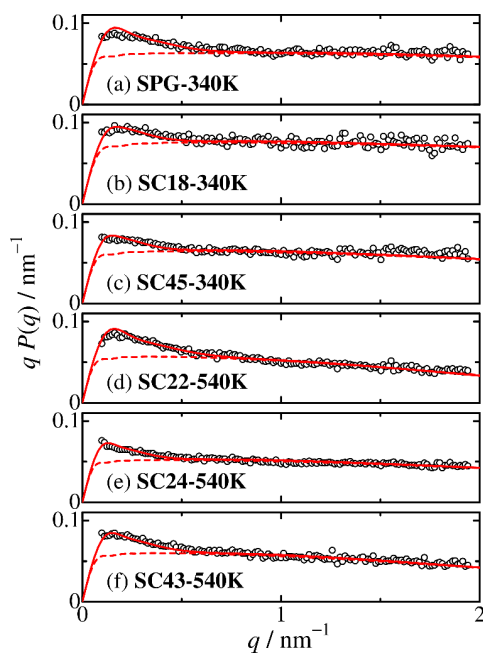


Fig. 3. Holtzer plots of (a) **SPG-340K**, (b) **SC18-340K**, (c) **SC45-340K**, (d) **SC22-540K**, (e) **SC24-540K**, and (f) **SC43-540K** in 200 mM aqueous NaOH including 10 mM NaCl at 25 °C. Solid curves indicate the theoretical values for the touched-bead wormlike chain with the parameters listed in Table 2. Dashed curves are the theoretical values for the rod limit ($\lambda = 0$).

Table 2

Wormlike chain parameters of SPG and sclerox samples in 200 mM aqueous NaOH including 10 mM NaCl

Sample	h / nm (L / nm)	λ^{-1} / nm	d_b / nm
SPG-340K	0.10 (47 ± 2)	13 ± 2	0.8 ± 0.3
SC18-340K	0.10 (40 ± 3)	17 ± 2	0.7 ± 0.3
SC45-340K	0.10 (47 ± 2)	18 ± 3	0.9 ± 0.3
SC22-540K	0.12 (52 ± 2)	12 ± 2	1.6 ± 0.2
SC24-540K	0.09 (58 ± 3)	18 ± 3	1.0 ± 0.2
SC43-540K	0.11 (48 ± 2)	16 ± 2	1.4 ± 0.2

Kommentert [BEC3]: Would one not expect that the stiffness was closer to 16-18 since it is carboxylated?

The radius of gyration $\langle S^2 \rangle$ for the wormlike chain model is calculated by the Benoit-Doty equation [26, 31]

$$\langle S^2 \rangle = \frac{L}{6\lambda} - \frac{1}{4\lambda^2} + \frac{1}{4\lambda^3 L} - \frac{1}{8\lambda^4 L^2} [1 - \exp(-2\lambda L)] \quad (5)$$

The chain thickness effect is negligible for the current system. The calculated $\langle S^2 \rangle^{1/2}$ values with the parameters in Table 2 are slightly smaller (5–9 %) than the experimental data in Table 1, suggesting the effects on the molar mass distribution. We therefore concluded that both $P(q)$ and $\langle S^2 \rangle$ data for the current SPG and sclerox samples in 200 mM aqueous NaOH with 10 mM NaCl are consistently explained by the wormlike chain model.

The obtained λ^{-1} value for **SPG-340K** (13 nm) is much smaller than the triple helix ($\lambda^{-1} = 360$ nm) [18] but consistent with that for the single chain of curdlan, unbranched β -1,3-gluican, in aqueous 300 mM NaOH ($\lambda^{-1} = 12$ nm) reported by Nakata et al. [32]. This value is not very different from those for the other polysaccharide, cellulose and amylose in some solvent systems [23]. The helix pitch h per main-chain saccharide unit defined as $h \equiv LM_0/M_{w,1}$ listed in Table 2 is almost the same for all the samples investigated. Surprisingly, these are

Kommentert [BEC4]: Except for SC22-540K all carboxylated samples have higher Kuhn lengths than SPG (DS = 0). I guess this is reasonable because of an electrostatic contribution to the chain stiffness. Maybe add comment?

much smaller than the triplex ($h = 0.30$ nm) in solution [18], suggesting shrunken helical conformation is formed in the solvent due to intramolecular hydrophobic interactions. Such a small h value was also found for curdlan ($h = 0.18$ nm) in 300 mM aqueous NaOH [32] while much larger value ($h = 0.38$ nm) was reported from the crystal structure of the single chain curdlan [33]. According to our recent research, tightly winding helical structure with relatively short h value can be stabilized for polysaccharide derivatives when the side groups fit inside the helical main chain [34-37]. The shrunken helical structure for SPG and sclerox is thus most likely due to this specific interaction between the main chain and the side group. This single chain conformation may play an important role not only for the stability of the triple helical structure but also for the distinctive structure of renatured β -1,3-glucan such as macromolecular cyclization [5], complex with polynucleotides [9], and fibrous formation [38].

4. Conclusion

The single-chain conformation of native and carboxylated schizophyllan was investigated in 200 mM aqueous NaCl with 10 mM NaCl by means of SAXS measurements. While the chain stiffness is similar to that for the other single-stranded polysaccharides, that is, curdlan, cellulose, or amylose, the local helical structure is much shrunken due to the interaction between the main chain and side groups. This specific conformational feature is expected to be a key factor to elucidate the function of β -1,3-glucans, including the construction of gene delivery systems [39] and chemosensors [40].

Acknowledgment

We are grateful to Professor Takahiro Sato (Osaka Univ.) for fruitful discussion and to Dr. Noboru Ohta (Spring-8) for SAXS measurements. This work was partly supported by JSPS KAKENHI Grant Nos. JP17K05885 and JP18H02020. The SAXS data were acquired at

deleted: s

the BL40B2 beamline in SPring-8 with the approval of the Japan Synchrotron Radiation Research Institute (JASRI) (Proposal No. 2018A1124).

References

1. Capron I, Brigand G, Muller G. *Polymer* 1997;38:5289-95, [https://doi.org/10.1016/S0032-3861\(97\)00079-7](https://doi.org/10.1016/S0032-3861(97)00079-7).
2. Matsuda Y, Miyajima Y, Sato T. *Polym J* 2009;41:526-32, <https://doi.org/10.1295/polymj.PJ2008300>.
3. Oviatt HW, Brant DA. *Macromolecules* 1994;27:2402-08, <https://doi.org/10.1021/Ma00087a007>.
4. Matsuda Y, Okumura K, Tasaka S. *Polym J* 2018;50:1043-49, <https://doi.org/10.1038/s41428-018-0098-7>.
5. Stokke BT, Elgsaeter A, Brant DA, Kuge T, Kitamura S. *Biopolymers* 1993;33:193-8, <https://doi.org/10.1002/bip.360330118>.
6. Norisuye T, Yanaki T, Fujita H. *J Polym Sci, Part B: Polym Phys* 1980;18:547-58, <https://doi.org/10.1002/pol.1980.180180314>.
7. Kikumoto S, Miyajima T, Yoshizumi S, Fujimoto S, Kimura K. *J Agric Chem Soc Jpn* 1970;44:337-42, <https://doi.org/10.1271/nogeikagaku1924.44.337>.
8. Kikumoto S, Miyajima T, Kimura K, Okubo S, Komatsu N. *J Agric Chem Soc Jpn* 1971;45:162-68, <https://doi.org/10.1271/nogeikagaku1924.45.162>.
9. Sakurai K, Shinkai S. *J Am Chem Soc* 2000;122:4520-21, <https://doi.org/10.1021/ja0000145>.
10. Sletmoen M, Stokke BT. *Biopolymers* 2005;79:115-27, <https://doi.org/10.1002/bip.20340>.
11. Sanada Y, Matsuzaki T, Mochizuki S, Okobira T, Uezu K, Sakurai K. *J Phys Chem B* 2012;116:87-94, <https://doi.org/10.1021/jp209027u>.
12. Mochizuki S, Sakurai K. *Polym J* 2009;41:343-53, <https://doi.org/10.1295/polymj.PJ2008309>.
13. Kawahara K, Nishi Y, Nakamura S, Uchiyama S, Nishiuchi Y, Nakazawa T, Ohkubo T, Kobayashi Y. *Biochemistry* 2005;44:15812-22, <https://doi.org/10.1021/bi051619m>.
14. Terao K, Mizuno K, Murashima M, Kita Y, Hongo C, Okuyama K, Norisuye T, Bächinger HP. *Macromolecules* 2008;41:7203-10, <https://doi.org/10.1021/Ma800790w>.
15. Crescenzi V, Gamini A, Paradossi G, Torri G. *Carbohydr Polym* 1983;3:273-86, [https://doi.org/10.1016/0144-8617\(83\)90025-5](https://doi.org/10.1016/0144-8617(83)90025-5).
16. Coviello T, Maeda H, Yuguchi Y, Urakawa H, Kajiwarra A, Dentini M, Crescenzi V. *Macromolecules* 1998;31:1602-07, <https://doi.org/10.1021/Ma9716286>.
17. Yoshihara K, Okamoto S, Dobashi T, Oku H, Christensen BE, Sato T. *Carbohydr Polym* 2017;168:79-85, <https://doi.org/10.1016/j.carbpol.2017.03.038>.
18. Kashiwagi Y, Norisuye T, Fujita H. *Macromolecules* 1981;14:1220-25, <https://doi.org/10.1021/Ma50006a016>.
19. Yoshihara K, Sato T, Osumi T, Ulset A-ST, Christensen BE. *Carbohydr Polym* 2015;134:1-5, <https://doi.org/10.1016/j.carbpol.2015.07.049>.
20. Shimizu N, Yatabe K, Nagatani Y, Saijyo S, Kosuge T, Igarashi N. *AIP Conf Proc* 2016;1741:050017, <https://doi.org/10.1063/1.4952937>.
21. Glatter O, Kratky O. *Small Angle X-ray Scattering*. London: Academic Press, 1982,

22. Ishida S, Yoshida T, Terao K. *Polym J* 2019;in press, <https://doi.org/10.1038/s41428-019-0234-z>.
23. Jiang XY, Kitamura S, Sato T, Terao K. *Macromolecules* 2017;50:3980-85, <https://doi.org/10.1021/acs.macromol.7b00389>.
24. Burchard W, Kajiwara K. *Proc R Soc London, Ser A* 1970;316:185-99, <https://doi.org/10.1098/rspa.1970.0074>.
25. Nagasaka K, Yoshizaki T, Shimada J, Yamakawa H. *Macromolecules* 1991;24:924-31, <https://doi.org/10.1021/Ma00004a018>.
26. Yamakawa H, Yoshizaki T. *Helical Wormlike Chains in Polymer Solutions*, 2nd ed. Berlin, Germany: Springer, 2016, <https://doi.org/10.1007/978-3-662-48716-7>.
27. Nakamura Y, Norisuye T. Brush-like polymers. In: Borsali R and Pecora R, editors. *Soft Matter Characterization*: Springer Netherlands, 2008. pp. 235-86, https://doi.org/10.1007/978-1-4020-4465-6_5.
28. Nakamura Y, Norisuye T. *J Polym Sci, Part B: Polym Phys* 2004;42:1398-407, <https://doi.org/10.1002/polb.20026>.
29. Norisuye T, Tsuboi A, Teramoto A. *Polym J* 1996;28:357-61, <https://doi.org/DOI10.1295/polymj.28.357>.
30. Norisuye T, Fujita H. *Polym J* 1982;14:143-47, <https://doi.org/10.1295/polymj.14.143>.
31. Benoit H, Doty P. *J Phys Chem* 1953;57:958-63, <https://doi.org/10.1021/j150510a025>.
32. Nakata M, Kawaguchi T, Kodama Y, Konno A. *Polymer* 1998;39:1475-81, [https://doi.org/10.1016/S0032-3861\(97\)00417-5](https://doi.org/10.1016/S0032-3861(97)00417-5).
33. Okuyama K, Otsubo A, Fukuzawa Y, Ozawa M, Harada T, Kasai N. *J Carbohydr Chem* 1991;10:645-56, <https://doi.org/10.1080/07328309108543938>.
34. Terao K, Maeda F, Oyamada K, Ochiai T, Kitamura S, Sato T. *J Phys Chem B* 2012;116:12714-20, <https://doi.org/10.1021/jp307998t>.
35. Ochiai T, Terao K, Nakamura Y, Yoshikawa C, Sato T. *Polymer* 2012;53:3946-50, <https://doi.org/10.1016/j.polymer.2012.07.004>.
36. Jiang XY, Ryoki A, Terao K. *Polymer* 2017;112:152-58, <https://doi.org/10.1016/j.polymer.2017.02.012>.
37. Ryoki A, Kim D, Kitamura S, Terao K. *Polymer* 2018;137:13-21, <https://doi.org/10.1016/j.polymer.2017.12.063>.
38. Xu S, Xu X, Zhang L. *J Phys Chem B* 2013;117:8370-7, <https://doi.org/10.1021/jp403202u>.
39. Fujiwara N, Izumi H, Morimoto Y, Sakurai K, Mochizuki S. *Cancer Gene Ther* 2019;26:32-40, <https://doi.org/10.1038/s41417-018-0033-2>.
40. Tamano K, Nakasha K, Iwamoto M, Numata M, Suzuki T, Uyama H, Fukuhara G. *Polym J* 2019;in press, <https://doi.org/10.1038/s41428-019-0222-3>.

Graphical Abstract

Single-chain conformation of carboxylated schizophyllan, a triple helical polysaccharide, in dilute alkaline aqueous solution

Yu Tomofuji, Kazuto Yoshida,* Bjørn E. Christensen, and Ken Terao*

